

The Machine to End All Machines – Towards Self-Replicating Machines on the Moon

Alex Ellery
Department of Mechanical & Aerospace Engineering
Carleton University
1125 Colonel By Drive
Ottawa, ON K1S 5B6
613-520-2600 ext 1027
aellery@mae.carleton.ca

Abstract— We present the notion of a self-replicating machine for deployment on the Moon to leverage space colonization by exploiting its resources. The utility of self-replication cannot be understated – it offers the means to create an exponentially increasing general productive capacity on the Moon unconstrained by launch costs. Initially, we review the idea of physical self-replicating machines, emphasizing the universal constructor. The key to the universal construction mechanism necessary to realise self-replication is, we hypothesise, 3D printing. To date, 3D printing has been demonstrating its versatility in manufacturing structures, albeit of great sophistication. We briefly review 3D printing methods to date and suggest that fused deposition modeling and electron beam additive manufacturing offer a complete 3D printing capability suitable for deployment on the Moon. In our pursuit of a self-replicating machine, we have been working on 3D printing mechatronic components - electric motors, and to a lesser extent, electronics - as necessary steps to realizing 3D printing entire robotic machines in general (universal constructor) and 3D printers in particular (self-replicating machine). This 3D printer is essentially a core part of the payload for a rover vehicle which scours the lunar environment for the basic materials required for its own construction.

TABLE OF CONTENTS

1. INTRODUCTION.....	1
2. SELF-REPLICATING MACHINES	1
3. SELF-REPLICATING LUNAR ROVER.....	2
4. IN-SITU RESOURCES.....	5
5. 3D PRINTING AS UNIVERSAL CONSTRUCTION	6
6. 3D PRINTING ELECTRIC MOTORS	10
7. 3D PRINTABLE ELECTRONICS	11
8. CONCLUSIONS.....	12
APPENDIX: TURING MACHINES	12
ACKNOWLEDGEMENTS	13
REFERENCES.....	13
BIOGRAPHY	17

1. INTRODUCTION

Our objective is the implementation of self-replicating machines on the Moon with potential applications in constructing solar shields and solar power satellites as

solutions to our current global climate problems [1]. Self-replicating machines have been proposed to build solar power satellites (SPS), particularly photovoltaic arrays but without consideration of any mechanism to implement such a system [2]. The advent of self-replicating machines has the prospect of transforming space exploration by offering space mission concepts that are hitherto considered too expensive to pursue [3]. Self-replication offers exponential growth in general purpose productive capacity that may be exploited to create a vast extraterrestrial infrastructure at low cost.

We hypothesise that 3D printing of multiple materials – plastic, metal, glass and ceramic - offers a universal construction mechanism. With this in mind, we are approaching the problem of constructing a self-replicating machine from lunar resources from a bottom-up perspective. The lunar resources to which we are limited include regolith-derived volatiles (hydrogen and carbon compound), regolith itself (glass, silicon and iron) and asteroid-derived material from impact basins (nickel, cobalt, tungsten and selenium). Our self-replicating machine may be envisaged as a large mobile rover mounting bucket wheels, loading shovels, excavator buckets, drills, rockjaws, grinding tumblers, pump-driven unit chemical processors, 3D printers, milling tools, lathes, ball mills, extruders, assembly manipulators, etc. The key components of all these robotic devices are electric motors and supporting electronics on the assumption that structures will be relatively trivial to construct in comparison. By 3D printing motors and their electronic controllers, all forms of kinematic machinery can be constructed, i.e. any robotic machine including a universal constructor. We have been making significant progress in developing the first 3D printed electric motors and high capacity control electronics – this is described after reviewing a number of key concepts.

2. SELF-REPLICATING MACHINES

We briefly review the concept of self-replicating machines in the context of space exploration with an emphasis on hardware approaches. It has been suggested that self-replicating robots will be forthcoming from the artificial cells of synthetic biology before mechanical self-replicators emerge [4]. We disagree.

The original model of self-replication was the von Neumann self-replicating kinematic machine [5]. It comprised four major subsystems – (A) a universal constructing machine to manipulate material and construct what is specified by the computing machine C (akin to ribosomes); (B) a tape copier that copies the tape of the Turing machine C (akin to RNA/DNA polymerase); (C) a universal computing (Turing) machine to manipulate information on a program tape to instruct the universal constructor A (akin to repressor/depressor molecules); (I_{A+B+C}) a program tape containing a construction blueprint of the entire kinematic machine (akin to DNA). The key concept is the universal constructor, a machine that can build any machine specified by the instructions on the tape including a copy of itself, i.e. self-replication is derivative from universal construction. The von Neumann self-replicator overcomes the infinite regress problem by using the program tape in two ways – as interpreted instructions (by the universal constructor) and as uninterpreted instructions (by the tape copier). The universal constructor was envisaged as an abstract manipulator arm embedded in a sea of component parts. The manipulator inspects and acquires parts and assembles them according to the program stored on the memory tape. The selection of elementary parts (e.g. wire – NOR-gate – prismatic joint – rotary joint – connecting link – disconnect link) is assumed to be based on visual inspection which implies sophisticated image processing or some kind of visual markers to permit ready distinguishability of parts [6]. Once construction of the copy is complete, the memory tape is copied and inserted into the physical copy. A variation on the notion of inspecting and selecting parts in the environment is to self-inspect (self-program) and self-replicate on the basis of self-inspection rather than a pre-existing tape of instructions but there is no analogue of this capability in nature (it effectively implies Lamarckian evolution) [7].

The von Neumann kinematic model was later supplanted by the von Neumann self-replicating cellular automation (CA) model of which a hardware logic circuit version has been implemented [8]. The self-replicating CA model comprised 29 transition states including a quiescent state, 16 transmission states responsible for propagating excitations (OR gates), 4 confluence states (AND gates) and 8 sensor-based construction states. A pulser outputs a sequence of excitations when it receives an input (fan out); a decoder outputs an excitation when it receives a sequence of inputs (fan in). The hardware model comprised a set of “biodules” (comprising an FPGA computation unit with a dot matrix display unit) forming a small interconnected cellular array to emulate a small subset of the 100,000-200,000 cell array. However, this implementation yielded little insight into the problem of designing a physical self-replicating machine.

Hardware implementation of the kinematic model has also been attempted, primarily in an extraterrestrial context.

Thus, the idea of a self-replicating factory on the Moon is not new [9]. The 1980 NASA study proposed that a 100 tonne seed factory be deployed onto the Moon comprising eight subsystems. However, technology has advanced considerably since this study enabling further developments. The Chirikjian architecture comprised four subsystems [10]. It was realised through Lego Mindstorms kits supplemented with electrical and magnetic connectors to build a number of self-assembling robot prototypes constructed from coarse modules on a flat surface with printed ground lines and bar-coded landmarks for optical tracking. This is an example of environmental structuring to reduce “real world” complexities – this also occurs in biological systems in the form of cell membranes [11]. All biological cellular processes are pre-programmed genetically and regulated through homeostasis within a cellular enclosure to maintain a controlled intracellular environment. Similarly, the self-replicating machine must maintain a highly structured environment to minimise variance. The number of states in the Chirikjian-Suthakorn model was small with three basic line-tracking behaviours determined by four simple types of sensors (optical readers, contact sensors, metal detection sensor and touch sensor) [12]. The simplest configuration comprised seven modules – left and right motors, left and right wheels, manipulator wrist and passive gripper, and a microcontroller receiver – supplemented by assembly fixtures to force alignments. A second, more complex robot required three separate subassembly stations for chassis, left and right motor-track, and motorised gripper subassemblies. The motor-track assembly station included a hooking system while the motorised gripper assembly station included a ramp and both had controller units and light sensors. The assembled robot included the RCX microcontroller brick in the chassis assembly.

3. SELF-REPLICATING LUNAR ROVER

We have discussed self-assembling systems that assume prefabricated components and modules. A more complete architecture of a lunar self-replicating machine that incorporated in-situ resource utilization (ISRU) has been under development [13]. From a practical perspective, a real world system will involve a series of mining, chemical processing and factory processes: (i) material mining to extract mineral ores; (ii) chemical processing of ores to extract purified materials; (iii) forming of parts through manufacturing methods; (iv) inspection and assembly of parts in subsystems/systems. We shall address (iii) in this paper but will touch on some of the other aspects in this section. The three main lunar self-replicating architectures discussed here are summarized in Table 1. We submit that the Ellery architecture is the most complete of the three.

Table 1. Comparison of lunar self-replicating architecture

Freitas architecture [Freitas & Gilbreath 1980]	Chirikjian architecture [Chirikjian et al 2002]	Ellery architecture [Ellery 2016]
Paving robots to fuse regolith to form the factory foundation		Fresnel lens-based sinterer/melter
Mining robots based on front loader/bulldozer configuration for strip mining, cellar excavation and hauling of ore	Multifunctional robots with tooling for strip mining, excavation and transport of material within a 1 km ² area	Multifunctional tracked robot(s) with bucket wheels and biomimetic drill for regolith acquisition.
Thermochemical processing system to beneficiate, chemically extract purified elements using HF acid leaching	Thermochemical processing system to reduce mineral oxides	Magnetic/electrostatic beneficiation, thermochemical reduction of mineral oxides, FFC Cambridge process, Mond process
Fabrication system for casting and laser machining of aluminium, magnesium, steel, and basalt parts excluding electronics fabrication	Casting in sintered regolith for mechanical parts	Metal (various steels), silicone plastic, silica glass and silica/alumina 3D printing supplemented by milling including electrical components
Assembly system by manipulators with buffering through warehousing	Assembly system based on specialised rover-mounted manipulators for assembly of its constituent parts	Assembly system based on general purpose rover-mounted manipulators for assembly of its constituent parts
Computing and communications system to implement production planning, scheduling and operations (imported from Earth)	Excluded from self-replication process	Hardware neural net computing based on vacuum tube technology
Transponder triangulation network that functions to support self-localisation and navigation similar to GPS	Simple reactive behaviours based on simple electromechanical relay circuits	Hardware neural SLAM and neural feedback/forward models
Energy plant comprising an overhead canopy of photovoltaic solar cells to supply 2 MW	Solar energy generation, storage and distribution based on mirror-based solar concentrators for thermal energy, photovoltaic solar cells for electrical energy and fuel cell storage	Fresnel lens-based thermal energy generation with thermionic conversion for electrical energy
Dispersion by radial growth	Electromagnetic railguns to deliver offspring to long-distance random locations	Electromagnetic railgun/launcher

Mining robotics has been driven by two factors – the hazardous character of mining to human life and the challenges of extracting valuable material from diminishing grades of ore. Mining has adopted autonomous trucks, loaders and trains for material transport augmented by autonomous drilling and rock-breaking robotic machines. There are several methods for acquiring and transporting regolith: (i) rover vehicles; (ii) rail or tram vehicles; (iii) cable-driven buckets; (iv) conveyors; (v) pipelines; (vi) ballistic/rocket transport. Ballistic/rocket transport is generally reserved for transport to orbit from the lunar surface rather than local transport. The use of pipelines for regolith transport is considered inefficient. Cableway/dragline carriage system suspending a Stewart platform to lift and haul loads offers one approach to lunar excavation/construction [14]. The cableway comprised a cable track of braided metal wires, elevated supports at both ends of the track cable, and a trolley carrier (such as a

Stewart platform) that rides the track cable. The dragline excavator is a variation in which hoist cable suspends a bucket near vertically from a long truss boom and is pulled by a horizontal drag cable through the terrain to scoop up overburden. The cableway/dragline lends itself to automation more readily than rover vehicles by virtue of its simplicity of operation – hoist, drag and slew to move the bucket through a simple trajectory – while itself being positioned adjacent from the excavation site [15]. Railways for transport require considerable infrastructure so are generally discarded for lunar application. Although it has been suggested that rover platforms may not be the most efficient of excavation construction machines [16], most lunar mining concepts are in fact based around roving vehicles with wheeled or tracked chassis for transport, digging, excavating and levelling using a diverse set of attachments such as bulldozing blade, soil scoop, backhoe bucket, etc.

Rover vehicles, like cableways/draglines can be used for both excavation and transport but without the infrastructure overhead. Surface mining requires a multirole rover vehicle to perform several functions – ripper excavation, load-haul-dumping, drilling, etc. The self-replicating rover may be armed with a mechanism to acquire raw material for further processing. There are several methods of excavating regolith: (i) blade or bucket mechanism; (ii) drilling; (iii) explosives. We propose a bucket wheel system to scoop regolith [17] and a drill for subsurface acquisition of buried asteroid ores (average meteoritic component of lunar regolith is only 1%) [18]. We have considered mining aspects – in particular, excavation methods - in detail elsewhere [19].

Rotary drilling is often selected for extraterrestrial use by default for its maturity. However, vibratory percussion can reduce the penetration forces required (e.g. ultrasonic/sonic drilling system [20] which potentially favours the novel bio-inspired woodwasp design of percussive drill [21]. Compressed water vapour (assuming its abundance on the Moon) could provide drilling fluid for cooling and for the removal of cuttings. Self-casing thermal drilling eliminates the requirement for borehole casing and drilling fluid but would require prohibitive amounts of power. Drilling is required to emplace explosives for blasting of subsurface ores to fragment it into manageable units. Such buried explosives help to reduce the mechanical digging forces required for excavation. For the Moon, specific explosive charges of 0.04 kg/m³ of soft rock and 0.12 kg/m³ of hard rock are required [22]. Rather than chemical blasting with explosives, electrical blasting involves a fast discharge of electrical energy at an electrode from a capacitor bank into a small volume of electrolyte within rock. The electrolyte turns into a high pressure plasma which generates shockwaves in the rock. The keys to enhanced mining lie in increased capabilities in efficient mechanical rock-breaking mechanisms (mechanical rather than chemical explosives), borehole drilling and other mining machines [23].

We envisage a mobile factory system of around 10 tonnes with a robust traction system (such as the elastic loop mobility system [24, 25] which eliminates the need for paving robots. Furthermore, a tracked chassis provides high traction against reaction forces imposed on the rover by excavation devices. The Kapvik rover represents a very modest step towards such a rover with its reconfigurable chassis design, combined camera mast/soil scoop and sample canisters (Fig 1).



Fig 1. (a) Kapvik instrumented rocker-bogie chassis (actual); (b) Kapvik with elastic loop mobility system (model)

The rover must also include further processing which we assume occurs in a self-contained rover payload package – this eliminates the requirement for hauling and dumping of raw material. The ExoMars rover Pasteur payload comprises a robotic laboratory including a sample preparation and analysis system serviced by a central 6 DOF robotic manipulator with dexterous gripper [26] – it represents a rudimentary factory. The RESOLVE payload as an in-situ resource utilization package is more representative of what is required [27]. The rover must incorporate a thermochemical processing system more extensive than the RESOLVE payload including a Fresnel lens-based solar power source, fractional distillation column for condensing regolith volatiles, foundry for smelting minerals and FFC Cambridge electrolysis cell for reducing mineral oxides and purifying metals [28]. The ubiquitous nanophase iron grains impregnating all lunar dust particles impart high magnetic susceptibility to lunar dust. This high magnetic susceptibility may be exploited through microwave processing as microwaves couple with iron strongly [29]. It offers high heating rates ~1000^o/min up to 2000^oC but at a cost of high electrical power consumption. The energy plant is based on Fresnel lens concentrators supplemented by thermionic conversion and flywheel energy storage.

We propose a 3D printing suite as the centrepiece of the rover payload based on fused deposition modelling (for silicone plastic and ceramic/glass precursors) (such as a RepRap derivative [30], electron beam freeform fabrication (for iron, nickel, cobalt, silicon, tungsten, selenium, and possibly aluminium/magnesium) [31] and Fresnel lens-based sinterer/melter (for ceramic processing) supplemented by integrated milling. 3D printing introduces the notion that subtractive processes can be reduced (but not eliminated entirely). 3D printed moulds retain the capacity for rapid casting of numbers of parts. Electron beam fabrication is selected over laser fabrication to eliminate difficulties in replicating a laser.

Although assembly is minimised through 3D printing, a revolte manipulator may perform compliant assembly with special consideration on latching/joining mechanisms (such as the remote centre compliance mechanism [32]. The rover assembly payload may be configured into a reconfigurable workcell built around standard component modules – actuators/sensors, kinematic connectors, tooling and fixtures

– that may be assembled into robotic machines with specific geometries for desired tasks [33]. The workcell may comprise a 7 DOF serial manipulator to pick and place a workpiece (assembly task) and a 6 DOF parallel manipulator to machine the workpiece linked by a 1 DOF linear conveyor between them. Tooling can be interchanged through standardise interfaces.

The issue of closure of materials, energy and information is essential to ensure that self-replication can occur - the machine must mine, process, fabricate and assemble every material, part and system from which it is constituted [34]. It was envisaged that certain complex or exotic parts could be exempted and supplied as “vitamins” from Earth – electronics, instruments, motors, etc. Our approach to solve the closure problem is to (i) minimise the number of materials and extraction complexity required; (ii) implement generic processing (FFC Cambridge process) and manufacturing (3D printing) techniques to minimise machinery; (iii) demonstrate universal construction through 3D printing of mechatronic components (electric motors, sensors and neural network hardware) [35]; (vi) to build the self-replicator from the ground up based on function through simplicity (rather than optimisation) and subject to the constraints of the lunar environment.

Large environmental variances such as those encountered by robots engaged in mining and manufacturing require behavioural flexibility typically associated with AI capacities. A few short years ago, this would have been considered the weakest aspect of any robotic lunar system. Today, however, AI has, after many years of lying fallow, been spurred by developments in deep learning systems with applications in robotic mining and lights-out manufacturing, amongst others. The central task in manufacturing is planning of manufacturing task schedules and sequences. This may be treated as a search problem but it is NP hard so knowledge must be exploited. An assembly plan comprises a sequence of tasks subject to geometric constraints – it comprises an NP-complete problem but a range of constraints can drastically reduce the options [36]. A traditional expert system-based AI applied to automated manufacturing is one approach [37] such as the adoption of frames as objects organised in a semantic network [38].

Soft computing methods such as neural networks and other methods are also applicable [39]. Neural networks have been applied to many areas of manufacturing by virtue of their adaptability and robustness [40]. Elman recurrent neural networks have been used to implement a sequential controller for automated manufacturing [41]. This demonstrates that neural networks can implement causal relationships in a process plan. It is their learning ability that offers potential advantages over knowledge-based expert systems for intelligent manufacturing required in reconfigurable systems. Their applications cover almost all manufacturing domains including design, process planning, scheduling, process modelling and control, monitoring and diagnosis, quality assurance and robotic control systems.

Neural nets are ideally suited to learning the relationship between input manufacturing parameters such as depth of cut (d), feed rate (f), cutting velocity (v) and workpiece dimensions (D) and output manufacturing parameters such as cutting force (F), power consumption (P), temperature (T) and workpiece surface finish (r) [42]. Neurofuzzy approaches permit the use of both symbolic and subsymbolic techniques. In order to maintain system functionality, state measurements and estimation must be implemented using multi-sensor systems (pressure, temperature, forces, stiffness, vibration and wear) [43]. Most sensory feedback during manufacture of products is based on X-ray fluorescence and/or ultrasound to detect defects but simple displacement and force sensing can yield useful feedback to measure perturbations such as thermal deformations, mechanical deformations, tool wear and vibration chattering during machining. Product quality requires precision machining for good surface finish and measurement for closed loop control of tool forces. An alternative approach involves reduced intricacy in sensing and control (RISC) which advocates minimal arrays of optical sensors for local sensing, simple parallel jaw grippers, passive remote centre compliance and environmental fixtures for complex manufacturing operations [44]. The key is the decomposition of complex operations into multiple simple robotic operations. Petri net can decompose complex scheduling problem into more tractable subproblems: $PN=(P,T,I,O,M,K)$ where P =set of places, T =set of state transitions, $P \cup T \neq \emptyset$, $P \cap T = \emptyset$, $I:P \times T \rightarrow N=\{0,1,2,\dots\}$, $O:P \times T \rightarrow N$, $M:P \rightarrow N$, $K:P \rightarrow N$. The ultimate goal is to replace sensors by constraining motion through friction using a tightly structured environment [45]. It is not currently clear how far such sensorless approaches can ease AI complexity but a combination suggests an effective approach. Having presented a brief plausibility argument, we do not address these AI aspects further here.

4. IN-SITU RESOURCES

We take the view that any kinematic machine (or robot) is a configuration of motors – be it a rover vehicle, manipulator, drill, excavator, 3D printer, milling machine, etc. Manufacture of the motor is the core of the self-replication process. In order to fabricate structures, motors and electronics, we have devised a minimal list of functional materials that can be extracted from the Moon or its NiFe meteoritic inventory (Table 2). It is worth noting that on Earth, Pt group metals are mined from ores with only 7 ppm metal and these materials have similar or greater concentrations on the Moon.

Table 2. Minimal set of functional lunar-derived materials

Functionality	Lunar-Derived Material
Tensile structures	Wrought iron

Compressive structures	Cast iron
Elastic structures	Steel springs/flexures Silicone elastomers
Hard structures	Alumina
Thermal conductor straps	Fernico (e.g. kovar) Nickel
Thermal insulation	Glass (SiO ₂ fibre) Ceramics such as SiO ₂
High thermal tolerance	Tungsten Alumina
Electrical conduction wire	Fernico (e.g. kovar) Nickel
Electrical insulation	Glass Ceramics (SiO ₂ , Al ₂ O ₃ and TiO ₂) Silicone plastics Silicon steel for motors
Active electronics devices (vacuum tubes)	Kovar Nickel Tungsten Fused silica glass
Magnetic materials	Ferrite Silicon steel Permalloy
Sensory transducers	Resistance wire Quartz Selenium
Optical structures	Polished nickel Fused silica glass
Lubricants	Silicone oils Water
Combustible fuels	Oxygen Hydrogen

Substitution of steel by aluminum and plastic on Earth is not necessary on the Moon, but the FFC Cambridge process offers the capability of a wide range of metals from mineral oxides. We wish to implement an industrial ecosystem in which the consumption of materials and energy is optimized by minimising waste, and the waste of one process becomes the raw material for other processes. Minimisation of waste is also a Toyota production system philosophy that seeks to maximise return on investment. Minimisation of consumption is the key to developing a self-sustained industry of which a self-replicating machine is an exemplar. Recycling is an attempt towards this though recycling requires energy input and is never 100% efficient [46]. The self-replicating machine provides such a 100% recycling capability through the construction of its daughter products (itself a form of self-repair).

5. 3D PRINTING AS UNIVERSAL CONSTRUCTION

We briefly review 3D printing techniques to assess their suitability for extraterrestrial deployment (though we do not consider issues invoked by partial gravity on planetary surfaces). One of the most important issues concerns the use of organic binder which may require a complex manufacturing process necessitating its import from Earth. Although Earth-imported reagents that are recycled may be tolerated, consumption of Earth-imported materials into products is not. Furthermore, in terms of a self-replicating machine, re-use of the same device for multiple purposes provides an efficiency of both material and manufacturing processes – in particular, we focus on vacuum tube-derived technology based on the electron gun. Conventional subtractive manufacturing involves removing material from a stock – it may be by machining, laser, electric discharge, etc. Prior to the spread of additive manufacturing, material cutting was the principal operation in 86% of flexible manufacturing system (FMS) operations. CNC machining is an example of subtractive manufacturing which employs a 3 or 5 DOF manipulator with tooling and supported by fixtures. Subtractive manufacturing processes are highly reliant on electric motors to drive hard tools to perform drilling, milling, sawing and laser/electron beams. Conventional forming processes are also highly reliant on electric motors. Material joining is reliant on thermal energy sources like electric arcs, burning gases and laser/electron beams.

Additive manufacturing (henceforth synonymous with 3D printing) is enabled through the digital STL file format which permits slicing of the CAD model into a series of cross sectional layers of arbitrary thickness for direct manufacture through CAM. 3D printing introduces new capabilities – it can fabricate parts with a wide range of complex geometries without the tooling, fixtures, jigs and moulds that characterise subtractive manufacturing methods and with fewer manufacturing steps [47]. This is unlike subtractive manufacturing which requires multiple process tools such as casting, machining, welding etc. Furthermore,

fewer components for assembly yield materially more efficient structures by minimising joinery and unnecessary material with mass savings of 40-90%. Additive manufacturing offers the potential for enormous savings globally by eliminating material waste (swarf, etc) with associated reductions in greenhouse gas emissions [48]. Excess material is readily recycled at the source. It enables simplification of structural design and fewer parts count by integrating parts, i.e. minimising material, shape and functional complexity [49]. In terms of sustainability, a high degree of recycling at product end-of-lifecycle is conceivable. The reconfigurability of 3D printed products offer advantages of distributed manufacturing close to point of demand with digital design files transported electronically, i.e. reduce physical transport if the material source is widespread [50] - manufacturer and consumer are merging into the same agent. This has been pioneered by the Fab@Home factory system and the RepRap 3D printer which could conceivably develop beyond the enthusiast or hobbyist [51]. All cases of 3D printing involve a Cartesian robot configuration in which a deposition head is moved in a 2D planar pattern that outlines the layer geometry, and a work platform which is moved in the vertical direction to permit consecutive layer upon layer construction. Hence, like subtractive manufacturing, it is also reliant on electric motors, thermal heating and laser/electron beams. There are several major approaches to 3D printing.

Stereolithography (SLA) was the first 3D printing technique developed by Chuck Hall in the 1980s to exploit digital CAD models. It is based on layer-by-layer construction of a photosensitive resin (such as Cibatool[®] SL 5170 resin) using UV light. A low power UV laser is directed onto a thin layer on the surface of a vat of liquid photosensitive polymer to polymerise it by cross-linking into a solid resin layer. The UV laser spot is controlled by mirrors to trace out the desired cross sectional pattern on the liquid photopolymer which hardens into a solid on exposure to UV. The platform mounting the part is depressed to submerge the solidified layer until a layer-thickness of liquid resin covers the solid layer. This liquid layer is then subjected to another cycle of UV laser treatment. UV light repeatedly solidifies thin layers so that a 3D part of resin is constructed layer-by-layer. It can achieve high resolution layering ~5-20 μm and a horizontal precision of ~1-10 μm . Such high resolution is achievable because it does not create a melt pool unlike most other 3D printing processes. It does require support structures for overhangs which are subsequently removed from the finished part. SLA is limited in the material choices (UV photopolymers) available. It is not considered suitable for extraterrestrial use due to its material limitations.

Laminated object manufacturing (LOM) bonds thin solid sheets of paper, metals, plastic or composite coated in a thermal adhesive under pressure and heat. A laser cuts the material of each layer to the desired cross sectional shape. The laser focus and velocity is controlled for depth to ensure that only one layer is cut. This process proceeds layer-by-

layer. It is thus a combination of additive (layering) and subtractive (laser cutting) manufacturing techniques. However, LOM layers are subject to warping in the z-direction. Ultrasonic consolidation can 3D print multi-material metal parts from dissimilar metal foils such as aluminum, steel and inconel with embedded ceramic fibres with high internal bonding integrity [52, 53]. It requires a post-process milling stage which may be integrated into the additive manufacturing device. The layering in LOM requires prefabricated sheet feedstock with a complex assembly process which excludes it from further consideration for extraterrestrial use.

Fused deposition manufacturing (FDM) melts a thin filament of thermoplastic which feeds into an extrusion head which deposits a thin layer of plastic onto a substrate. The plastic is heated to 1°C above its melting point in the extrusion head so that it solidifies rapidly after extrusion to form 50-250 μm layers. Each layer is deposited consecutively to build the 3D part. Due to cold welds between layers, delamination can occur if the temperature fluctuates. The most commonly used thermoplastics are acrylonitrile butadiene styrene (ABS), polylactic acid (PLA), nylon and more recently silicone plastics (siloxanes). FDM is a 3D printing technique that offers versatility despite being restricted to plastics. Its application to silicone plastics is of particular value for extraterrestrial employment as siloxanes are radiation resistant and have wide temperature tolerance.

Of particular interest with respect to FDM are preceramic polymers which include silicone-based polysiloxanes [54]. The high melting point of most ceramics makes their direct casting and 3D printing very difficult at best. Furthermore, their high brittleness renders them prone to thermal cracking if large thermal gradients exist. Pyrolysis of polysiloxanes such as PDMS at 350-1000°C or above can yield highly quality SiO₂ films with the evolution of CO₂. This permits thermal preforming of the polymer prior to its conversion to ceramic which then has an ultrahigh temperature tolerance up to 1600°C. Above 1400°C, silica forms its high temperature cristobolite form which exhibits piezoresistivity. Iron-containing polymer-derived ceramics can form ceramics with magnetic properties. Combining siloxanes (Si-O-Si) with silazanes (Si-N-Si) results in SiOCN ceramics after pyrolysis at 1000°C in a noble gas environment [55]. The requirement for thin thickness under 3 mm dictates the employment of lattice and honeycomb structures capable of surviving high temperatures. The application of UV radiation in the presence of oxygen (forming ozone) can potentially reduce polysiloxanes such as PDMS to silica at room-temperature [56]. This process is limited to a surface film of 20-30 nm with potential applications in microelectronics. The UV-exposed layer can be 30-100 μm which is compatible with 3D printing layers. On the Moon and Mars, ambient solar UV flux can be exploited in this manner to create ceramics from siloxanes after 3D printing at low temperature.

Inkjet 3D printing is derived from dot-matrix printing – a solute is dissolved in a liquid solvent (ink) and the solution is sprayed through a nozzle. It deposits liquid droplets of a polymer binder (ink) over a powder bed of particles (usually metal or ceramic) to form a composite layer of the desired shape. The ink dries through evaporation of the solvent to bind the particles into a solid horizontal patterned layer. A new layer of particles is then deposited over the hardened layer followed by the liquid binder. The viscosity, inertia and surface tension of the ink determines the droplet behaviour as represented by the Reynolds number Re (ratio of inertial to viscous forces), Weber number We (ratio of kinetic to surface energy) and Ohnesorge number Oh (relative importance of viscous to surface forces):

$$Oh = \frac{\sqrt{We}}{Re} = \frac{\eta}{\sqrt{\rho\sigma d}} \quad (1)$$

where $Re = \frac{\rho dv}{\eta}$, $We = \frac{\rho dv^2}{\sigma}$, v =fluid velocity, η =dynamic viscosity, d =droplet diameter, ρ =fluid density, σ =surface tension. If $Oh > 1$, nozzle clogging will occur; if $Oh < 0.1$, multiple droplets will result. The jetting condition is thus $1 < Oh < 0.1$. Inkjet 3D printing can bind most types of powder but it offers limited parts density. The requirement for an imported binder renders it unsuitable for extraterrestrial use.

Prometal 3D printing is a variation on inkjet 3D printing in which a powdered metal, ceramic or composite (most commonly steel particles) is deposited onto a substrate followed by spraying with a binder from a nozzle tracing the desired cross sectional pattern. After the 3D part has been constructed layer-by-layer, it is fired at elevated temperature ~ 170 - 180°C for 24 h to strengthen the binding to yield a 40% porous 3D part. The part may then be infused with bronze powder at 1100°C to form an alloy of 60% steel and 40% bronze for near full densification. Tungsten carbide particles sintered with zirconium copper have been 3D printed into rocket nozzles using this technique. The previous argument applies.

Multiphase jet solidification uses low melting point alloys (such as tin-bismuth with a melting point of 180°C) or ceramic powder-polymer binder (typically in a 50%:50% ratio) paste which is forced from a nozzle to create parts layer-by-layer [57]. The polymer binder impregnated by ceramic particles may be heated and extruded under low viscosity flow to sequentially build each layer which is cooled before the next layer is applied. Stainless (316L) steel powder may similarly mixed with the polymer binder to extrude at low temperature but evaporation of the binder results in 30% volume shrinkage and the part still requires subsequent high temperature sintering. The previous argument applies.

Most work to date on metal additive manufacturing has been focussed on Ti6Al4V though many alloys can be employed. For metal 3D printing, there are three main approaches for inputting metal – powder bed, powder feed and wire feed

[58]. Powder bed fusion offers superior tolerance and finish while wire feed offers rapid deposition rate. There is a correlation between microstructure, processing parameters and materials properties – the microstructure of powder-generated material is finer than that of wire-generated material due to the larger melt pool and consequent slower cooling of wire feeding. In powder bed fusion, a powder is raked over the work area for subsequent thermal processing. In powder feed, the powder is deployed from a nozzle with gas onto the work area for subsequent thermal processing. In wire feed, the energy source – laser beam, electron beam or plasma arc – impinges on the wire to deposit molten beads onto the work area. The optimal configuration for superior surface finish is to position the wire at the leading edge of the melt pool through front feeding. In terms of power delivery, there are three main thermal power sources – selective laser sintering/melting (SLS/M techniques pioneered by EOS and Renishaw respectively), electron beam melting (EBM pioneered by ARCAM) and arc welding. They are all selective sintering/melting methods that impose a localised heat source on the material.

Welding is a joining process which melts base metal for fusion supplemented by a filler metal (as opposed to soldering and brazing which melt another metal at lower temperature). There are several common forms of welding but the three most appropriate for extraterrestrial deployment include: (i) oxyacetylene welding uses acetylene fuel ignited in oxygen to weld and cut metal (acetylene may be manufactured readily from Martian resources); (ii) TIG (tungsten inert gas) welding uses a tungsten electrode to generate an electric arc and an Ar/He shielding gas to weld; (iii) special welding techniques for high energy density, deep welding including laser beam welding (in air or in vacuo) and electron beam welding (in vacuo). The TIG welding torch employs tungsten electrodes in common with vacuum tube devices (see later). We do not consider welding further here other than to note that pairing of electron beam welding with electron beam additive manufacturing (both based on vacuum tube-based devices) and laser beam welding with selective laser sintering/melting offer combined additive and subtractive techniques.

In powder beds, the commonest approach to metal additive manufacturing, the laser or electron beam selectively thermally fuses a pattern on the powder bed layer-by-layer, yielding fully dense metal components with relatively high precision [59]. The powder bed is maintained in an inert gas environment such as Ar (for laser) or vacuum $\sim 10^{-4}$ - 10^{-5} mbar (for electron beam) environment in an enclosed chamber. The laser or electron beam scans over the powder bed to sinter or melt the particles in a 2D cross section pattern. Conductive heat flow from a rapid scanning laser or electron beam onto a solid material is determined by [60]:

$$\frac{\partial T}{\partial x} - D\nabla^2 T = \frac{Q}{c_p} \quad (2)$$

where D =thermal diffusivity, c_p =specific heat/unit volume, T =temperature, $Q = \frac{P(f)}{2\pi r^2 \lambda}$ =power density, $P(f)$ =Gaussian beam power distribution function, r =beam spot radius, x =material thickness, λ =absorption length (related to layer thickness). Power density is determined by the beam energy given by $E = hf$ for the laser and $E = \frac{1}{2}mv_e^2$ for the electron beam respectively. Rapid heating and cooling rates of $\sim 10^4$ K/s at solid/liquid interface in the melt pool is typical. Once the solidified layer is complete, the work platform is depressed one layer thickness and a roller spreads another layer of powder onto the solidified layer. The unsintered powder of the underlying layer acts as support for the overlying layer thereby permitting overhangs without dedicated support structures. The process is repeated layer-by-layer until the 3D part has been constructed. The 3D part may be subjected to post-processing procedures such as machining, shot peening, heat treatment, hot isostatic pressing, etc.

Selective laser sintering (SLS) uses a high powered laser (usually CO_2 laser) to sinter a bed of powdered polymer, metal, ceramic or glass particles or combinations thereof into a hardened solid. Solidification of powder occurs without melting. In particular, steel, nickel, cobalt, inconel, titanium, intermetallics, alumina, silica, zirconia, PZT and PEEK are commonly printed using SLS. SLS focusses a laser to sequentially sinter layers of fine powder into patterns traced out by the laser. After each layer is sintered, a fresh layer of powder is rolled sequentially onto the powder bed. The residual stress is dependent on the material (especially coefficient of thermal expansion and elastic modulus), part height and laser processing conditions (including tool path). The major laser processing parameters are laser power P , scan speed v , beam size, hatch distance h between laser tracks and powder layer thickness d . Laser-based deposition thickness for a Gaussian beam profile is given by:

$$h = \frac{R_0 r t \sqrt{\pi}}{\sqrt{\pi r + 2(vt)}} \quad (3)$$

where r =laser spot radius, R_0 =diffusion-limited axial growth rate, v =scanning speed, t =process time. The effects of laser parameters are integrated into the volumetric energy density factor (kJ/mm^3):

$$VED = \frac{P}{vhd} \quad (4)$$

The sintering laser is typical 200-1000 W for metals and must deliver $< 10 \text{ MW/cm}^2$ for optimal processing. Laser AM can print with 20-50 μm thick layers depending on the powder size (which determines the stair stepping effect), dimensional accuracy of $\pm 50 \mu\text{m}$ and a surface roughness of $\sim 10\text{-}15 \mu\text{m}$. Sintered parts are near fully dense but laser scanning is slow with a build rate of 5-20 cm^3/h but multiple sets of lasers can increase this rate. Glass/carbon/metal fibre reinforced composites with plastic or metal matrices (such as steel, Ti alloys, and Ni-Co super-alloys) may be 3D

printed offering higher strength, stiffness and stability than traditional forging/machining methods.

In selective laser melting (SLM), the powder bed is heated just below the melting point of the material prior to melting to minimise thermal distortions of the new melted layer with the underlying solidified layer. The difference between laser sintering and laser melting is that in the latter, the powder is fully melted rather than partially as in the former. Melting of the powder results in greater densification compared with the small porosity from sintering but SLM still generally benefits from hot isostatic pressing (HIP). Laser melting permits processing of non-ferrous materials that are too viscous (which causes balling) for sintering. SLM involves high laser intensities delivering $\sim 10^{10} \text{ W/m}^2$ to the localised workpiece. Laser energy density is given by:

$$DE = \frac{2P}{\pi_0 v} \quad (5)$$

where P =transmitted laser power, v =laser scanning speed, r =laser spot radius. Ceramic processing requires high temperatures in excess of 1700°C . In multicomponent powder mixtures, the low melting point metal acts as binder while the high melting point metal acts as the structural component, typically with a small amount of additive to prevent oxidation [61]. The processing temperature is between the solidus and liquidus temperatures. Wetting of the structural metal by the liquid binder may be defined by the contact angle:

$$\cos \theta = \frac{\gamma_{sv} - \gamma_{sl}}{\gamma_{lv}} \quad (6)$$

where γ =surface tension between solid-liquid, solid-vapour and liquid-vapour interfaces. As $\cos\theta \rightarrow 1$, wetting increases. Viscosity of the molten material is given by:

$$\mu = \mu_0 \left(1 - \frac{1 - \phi_l}{\phi_m}\right)^2 \quad (7)$$

where μ_0 =base viscosity, ϕ_l =volume fraction of liquid, ϕ_m =critical volume fraction of solid above which viscosity is infinite. Heterogeneity in alloy mixtures can result requiring post-processing such as hot isostatic pressing. Despite its promise for multi-material additive manufacturing, we discard SLS/SLM techniques for extraterrestrial deployment for two reasons: (i) metal powders under partial gravity and vacuum conditions are difficult to control; (ii) lasers have poor energy conversion efficiencies.

Electron beam melting (EBM) is similar to SLM except that an electron beam replaces the laser, offering higher energy efficiency of 10-20% compared with the 2-5% efficiency of laser beams – this will be critical for extraterrestrial deployment. EBM can be powder or wire fed [62]. It can interact with many metal alloys including Ti, Al, steel, copper, Be, Co and Inconel alloys but cannot process electrical insulators. In mixed particles, melting temperatures range considerably from 1300°C for Inconel to

2500°C for Nb which affects pre-heat scanning strategies and melt scan beam currents. A heated tungsten cathode emits electrons that are focussed with two magnetic fields generated by the focus coil which acts a magnetic lens to focus the beam onto the powder bed ~0.01 mm diameter and the deflection coil which scans the beam over the powder bed. The electrons interact with the metal particles and melt them. The layer thickness is typically 50-200 µm. EBM is typically performed in two stages: (i) preheating stage preheats the powder bed with multiple passes at high scanning speed up to 40-60% melting temperature (700-900°C typically) to reduce thermal gradients and consequent residual stresses between layers; (ii) melting stage at low scanning speed to melt the powder. The main electron beam processing parameters are beam power, current, focus diameter, pre-heat temperature and layer thickness. For the electron beam, temperature of the bed is given by:

$$T \sim \frac{Q(1-R)}{\rho c_p v} \quad (8)$$

where $Q = \frac{IV}{v}$ = beam power density, R=reflectivity, ρ =material density, v =scan speed. Typical electron beam power is ~3 kW at 30-60 kV. EBM has a higher build rate of 100-2500 cm³/h but poorer surface finish than SLM. Within EBM manufacturing, measurements may be made by a scanning electron microscope (SEM) configuration. The SEM comprises an electron gun to generate an electron beam, a set of magnetic lenses to focus the beam and a focus platform, all encased in a high vacuum. Electron beam additive manufacturing, despite being limited only to metals, is a versatile technique based on vacuum tube-type technology.

Directed energy deposition methods of 3D printing (pioneered by 3D Systems) involve melting of material as it is being deposited. An example is laser engineering net shaping (LENS pioneered by Optomec) which uses a high power laser (500 W – 5 kW) to sinter or melt metal powder particles which form consecutive layers vertically on a substrate build a 3D part. It requires the part to be cut from the substrate and requires post-processing. It is a variant on the SLM technique so the same criticisms apply.

Amorphous ceramic structures have been fabricated using additive LENS from lunar regolith simulant (primarily plagioclase with supplementary olivine and pyroxene particles of 50-150 µm) [63]. The process parameters were laser power of 50 W (laser spot size of 1.65 mm giving an energy density of 2 J/mm²), scan speed of 20 mm/s and powder feed rate of 12.4 g/min. The printed glassy material had a hardness of 500 Hv similar to soda lime glass (550 Hv) using those parameters. This demonstrates the viability of 3D printing of lunar regolith for habitat and other structures as an alternative to lunar contour crafting and 3D-shape which both use a large extrusion nozzle to lay a viscous mixture of concrete and regolith/binder respectively [64].

The chief problems in 3D printing have been in process control for high gradient thermal cycles and their effects on mechanical properties, and higher dimensional accuracy for reduced surface roughness. It is the lack of quality assurance by monitoring process control in additive manufacturing that has hampered surface roughness and other deficiencies in the build – feedback loops with adequate sensors is essential [65]. Stair-stepping between layers is determined by the layer resolution which is determined by process control. Balling occurs when the melt forms spheres that exceed the layer thickness resulting in non-uniform material distribution. Balling may be reduced at heat inputs of 1400-1700 J/mm³. A feedback system can provide closed loop control of dimension during deposition using sensors to extract melt pool information and adjusting input processing parameters. In melting, Marangoni convection driven by surface temperature gradients of the melt pool affects the quality of the melt pool [66]. Camera imaging of the melt pool can detect imperfections and measure dimensional inaccuracies. In particular, accurate distance measurements are required – photodiode sensors and/or electromagnetic sensors are ideal. Temperature gradients may be identified by pyrometers or infrared cameras protected by ZnSe window. However, the range and mix of sensors may be much enhanced (such as X-ray spectroscopy) especially with data fusion. Integration of sensors, software and communications is required for seamless autonomous control of industrial machines and processes. However, these approaches are still in developmental stages though they show much promise.

6. 3D PRINTING ELECTRIC MOTORS

Whereas the 1980 NASA study considered that electric motors and electronics are complex and should be imported from Earth, Chirikjian et al (2002) suggested that electric motors might be assembled from cast components in-situ [67]. Furthermore, electromechanical relays operate on a similar principle and using similar components as electric motors. A network of manufacturing tools (cyclic fabrication) – laser machining, assembly, casting, hot wax vacuuming and electroforming - has demonstrated the fabrication of a brush “air” DC motor from polyurethane, silicone resin moulds, sacrificial wax moulds, solder alloys, and metal salt solutions of copper and nickel [68]. The motor comprised 15 cast plastic parts (6 coil plates, 7 magnet disks, 1 commutator shaft, 1 baseplate), 4 cast Rose’s metal commutator rings, 8 brass brushes, 6 magnetic steel yoke pieces, 42 NdFeB magnets and extruded Rose’s metal wires. The motor was complex in construction and required complex machinery to fabricate.

The approach we are exploring is to vastly simplify electric motor construction through 3D printing using more robust materials. We have been striving towards 3D printing electric motors [69, 70] as a corollary to the theorem that 3D printing supplemented with milling constitutes an universal construction mechanism. We have made progress in 3D

printing DC electric motors including rotor core, coils and stators. This has involved 3D printing in metals and plastic. The motor core comprises magnetically soft material (silicon steel) powder impregnating an insulating resin binder of PLA has been 3D printed by FDM (Fig 2).

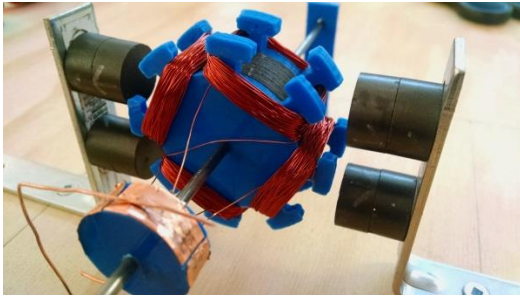


Fig 2. 3D printed iron-impregnated PLA-based rotor for a DC motor

We have photolithographically printed the electrical coils in a pancake motor test configuration which has successfully demonstrated the elimination of wire windings (Fig 3). Photolithography is of course a variation on stereolithographic 3D printing. We are in the process of integrating the two elements – 3D printed rotor and lithographically printed coils – into a hybrid fully-printed rotor.

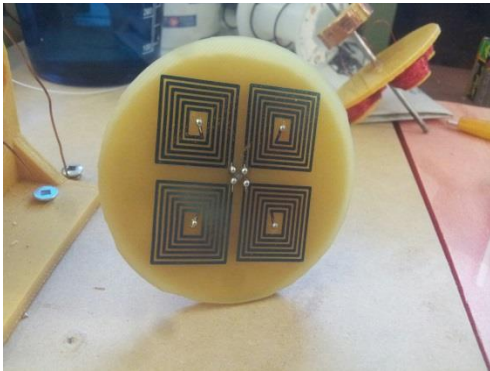


Fig 3. Photolithographically-printed coils

We have also 3D printed electromagnetic iron alloy (by SLM) for the stator magnets with mixed success (Fig 4). Unfortunately, the stator field was only 3 G which was insufficient to generate torque on the rotor even with 900 turns of wire on the stator. However, we are exploring the use of a series of permanent magnet solutions – alnico, samarium-cobalt and rare earth alloys – to be 3D printed using EBM. Once the stator magnets have been successful, we shall integrate all three components into a fully 3D printed DC motor.

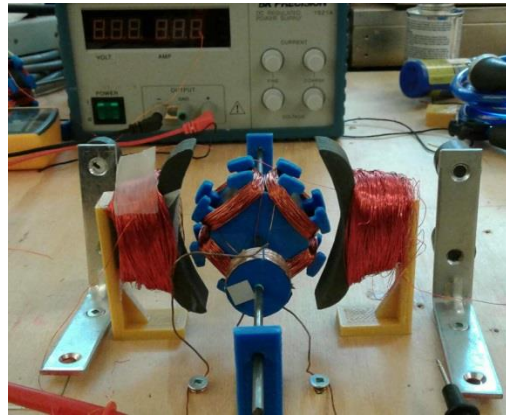


Fig 4. Unsuccessful electromagnetic stator

7. 3D PRINTABLE ELECTRONICS

Data processing and expert system functions to support self-replication is based on neural network architectures to implement AI capabilities [71] supplemented with offline training through deep learning [72]. This includes a neural SLAM capability [73] which eliminates the need for a transponder network.

We have been tackling the 3D printed electronics aspect from two directions. We have demonstrated the deposition of molten aluminum alloy strips directly onto silicone plastic substrates to demonstrate integrated multi-material compatibility (Fig 5).



Fig 5. Aluminium track on silicone plastic substrate

With further development, we will be able to print passive RC circuits. In our custom-made 3D printer, we shall utilise a modular motor unit to drive a rack-and-pinion in all three axes to form a Cartesian robot assembly. This bears

resemblance to the “modular production system” concept which comprised of two orthogonal horizontal modular prismatic links mounting a boring drill to a workpiece on a table actuated by a vertical prismatic link [74].

Our approach to computing with active devices however is based on vacuum tubes as the basis for hardware neuron circuits [75]. There is a complex trade-off between simple distributed electronics and microprocessor electronics whereby increased subsystems of reduced complexity enhance survivability in more complex environments [76]. This corroborates our approach to use distributed sets of neural network circuits rather than a centralised von Neumann architecture. We have been examining the use of analogue hardware neural network circuits as a new approach to computing (Fig 6).

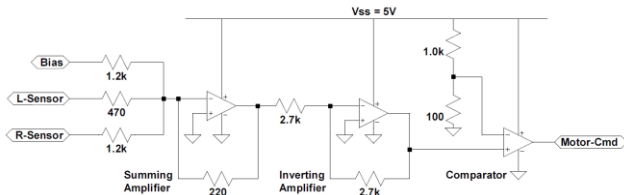


Fig 6. Analogue neuron circuit

We have demonstrated the efficacy of this neuron circuit on a desktop rover which used a two-neuron circuit to implement simple obstacle avoidance behaviour. The use of analogue neural circuits is motivated by the adoption of vacuum tubes as the core component of active electronics. Unlike solid state circuits, vacuum tubes can be constructed from lunar resources – glass, tungsten, nickel and kovar. There may be limits to their miniaturisation on the Moon, so neural net architectures offer logarithmic footprint growth with task complexity over the exponential growth implicit in traditional von Neumann architectures and their variants. We have yet to 3D print vacuum tubes but have demonstrated analogue hardware neural circuits controlling a desktop test rover. We are in fact exploring 3D printing of a magnetron as a macroscopic vacuum tube but this work is in its early stages. Nevertheless, this approach implements a direct implementation of the original Turing machine concept in which the read/write head is implemented as a 3D printing machine which outputs (prints) the neural circuit (computer program) to be implemented (see Appendix A for Turing machine tutorial).

8. CONCLUSIONS

The prospect of a self-replicating machine to develop and exploit extraterrestrial environments remains a significant challenge. Nevertheless, the first tentative steps have been taken and a solution and an implicit technological roadmap is visible. The lunar materials required that impose the ultimate constraints are understood. Core capabilities include 3D printing of electric motors and electronics as the key 3D printing of entire robotic machines including 3D printers (universal constructors) and other supporting kinematic machines. Although this initial goal has yet to be

achieved, 3D printing of motors has almost been demonstrated but 3D printing of active electronics is less well developed.

APPENDIX: TURING MACHINES

Primitive recursive functions are a class of functions that may be computed mechanically, i.e. computable functions. A computable function may be defined as an algorithm (program) of a finite number of steps composed of a finite sequence of symbols from a finite alphabet of symbols but of arbitrary complexity. Computable functions may also be defined as those that are computable by a Turing machine. These are all equivalent definitions of computable functions. The last definition is a statement of the Church-Turing thesis which states that any computation can be performed by a Turing machine. A computable number is one that can be computed by a finite, halting algorithm, i.e. computable by a Turing machine. Computable numbers include all algebraic numbers and many transcendental numbers such as π and e . For any Turing machine, it is possible to construct an equivalent Boolean circuit that implements all its computations because Boolean circuits are equivalent to formulas of propositional calculus.

The Turing machine is a machine that encapsulates notion of the algorithm as a well-defined finite procedure of sequential steps that transform an input into an output. The Church-Turing thesis defines computation as a mathematically precise process embodied in the Turing machine. A Turing machine comprises three parts: (i) an infinitely long digital tape divided into consecutive cells containing symbols 0 or 1 – this is the stored program, and (ii) a finite state machine (movable read-write head) with q states that reads the tape as a sequence of inputs one cell at a time in either direction initiated from a start state q_0 and writes a new output sequence on the tape; (iii) a set of transition rules (program) that determines the next state of the read/write head. As the tape is read from and written to, the finite state machine alters its internal state. As an automaton, the Turing machine may be described by: $M=(Q,q_0,q_f, A,B,T, \delta)$ where Q =set of states, q_0 =initial state, q_f =final state, A =finite alphabet of input symbols, B =special blank symbol, T =finite alphabet of tape symbols, δ =transition function such that $\delta xT \rightarrow QxTx\{L,R\}$, L =move left, R =move right. The read write/head reads the an input symbol on the tape, overwrites the input symbol on the tape with the output symbol, and moves left or right to the next symbol. The sequence of transitions constitutes the computation. Often, the Turing machine concept has multiple tapes but they can be simulated by a single tape Turing machine. The tape may be likened to mRNA with each cell of the tape representing a codon. The transition function has been likened to biological translation represented by aminoacyl-tRNA pairing. The Turing machine computes a finite sequence of symbols until it reaches its halting state such that $Y=M(I)$ where Y =output string, I =input string, M =Turing machine. The computational automaton as a whole represents a ribosome.

There are several variations on the Turing machine. The Bernoulli-Turing machine is a deterministic Turing machine augmented by an information source modelled as heat bath.

The universal Turing machine (UTM) is a general Turing machine that can simulate any other Turing machine given the description of that Turing machine as an input on its tape. It can be an even more complex Turing machine at the cost of a fixed overhead to the program size and a polynomial decrease in computation speed. An important consideration is computational tractability. Computational complexity of an algorithm is defined as the time required for its computation on a Turing machine. The class of decision problems that can be solved by a Turing machine in polynomial time constitutes class P; PSPACE are problems that can be solved by a Turing machine with polynomial storage capability but may require exponential time; those that can be solved by a non-deterministic (probabilistic) Turing machine in polynomial time constitutes class NP. Soluble problems P are those soluble in polynomial time while problems NP are soluble in exponential time are considered to be insoluble (in a practical not theoretical sense) [77]. It is widely expected that $PSPACE \neq P$. Similarly, it is known that $P \subseteq NP$ but it is not known if $P=NP$ but it is suspected that $P \neq NP$. If, however, a single problem can be found in class NP that is also in P, then $P=NP$ would be proven.

There are many universal Turing machine concepts including small Turing machines such as the Minsky machine (with a 7-state read/write head and 4 symbol alphabet) and the one-dimensional cellular automaton Rule 110 [78]. At a hardware level, the UTM has to re-arrange its internal structure of switches to implement different algorithms. This introduces the key notion of a software algorithm differentiated from the underlying hardware. The modern computer, by virtue of its reprogrammability, is a universal Turing machine. In a von Neumann computational architecture, data is read and written by a central processing unit (CPU) by fetching data to and from memory. Similarly, a dynamical system is computationally universal if it can be programmed to perform any digital computation [79]. Computation may be represented as ordinary differential equations of the form $\frac{dx}{dt} = f(x)$ which converge to attractors (fixed points, limit cycles or chaotic attractors) as their computational outputs, e.g. the Hopfield neural networks relaxes to the solution of optimisation problems in which the solution is that state which minimises a cost function E by finding the local minimum from gradient flow $\dot{x} = -gradE$ [80]. Hence, the equivalence of dynamical systems and Turing machines dictates that either can be used to represent the other and that all cause/effect relations can be expressed either through deductive logic or numerical computation. Analogue neural networks represent such dynamical systems.

There are limits to the Turing machine – they suffer from the halting problem whereby it is impossible to determine in

advance whether a particular program will halt with a computed output – the unsolvability of the halting problem denies the existence of any general algorithm that can determine whether a given computation will halt or not, i.e. this halting problem is undecidable. For example, a search for a counterexample to disprove Goldbach’s conjecture (that every even number greater than 2 is expressible as the sum of two primes) will find a counterexample if it exists but will continue forever if it does not.

ACKNOWLEDGEMENTS

The author thanks the National Science & Engineering Research Council for part funding this project.

REFERENCES

- [1] Ellery A (2016) “Solar power satellites for clean energy enabled through disruptive technologies” *Proc 23rd World Energy Congress (Award Winning Papers)*, Istanbul, Turkey, 133-147
- [2] Lewis-Weber J (2016) “Lunar-based self-replicating solar factory” *New Space J* **4** (1), 53-61
- [3] Ellery A (2017) “Space exploration through self-replication technology compensates for discounting in net present value cost-benefit analysis” *New Space J* **5** (3), 141-154
- [4] Cho A (2007) “Making machines that make others of their kind” *Science* **318**, 1084-1085
- [5] von Neumann J and Burks A (1966) *Theory of Self-Reproducing Automata*, University of Illinois Press, Champaign, Ill
- [6] Stevens W (2009) “Parts closure in a kinematic self-replicating programmable constructor” *Artificial Life & Robotics* **13** (2), 508-511
- [7] Freitas R & Merkle R (2004) *Kinematic Self-Replicating Machines*, Landes Bioscience, Texas
- [8] Beuchat J-L & Haenni J-O (2000) “von Neumann’s 29-state cellular automaton: a hardware implementation” *IEEE Trans Education* **43** (3), 300-308
- [9] Freitas R and Gilbreath W, *Advanced Automation for Space Missions*, NASA Conference Publication 2255, Washington DC, 1980
- [10] Chirikjian G, Zhou Y, Suthakorn J (2002) “Self-replicating robots for lunar development” *IEEE/ASME Trans Mechatronics* **7** (4), 462-472
- [11] Sayama H (2002) “von Neumann’s machine in the shell: enhancing the robustness of self-replication process” *Artificial Life VIII* (eds. Standish, Abbas, Bedau), MIT Press, 49-52

- [12] Lee K, Chirikjian G (2007) "Robotic self-replication" *IEEE Robotics & Automation Magazine* (Dec), 34-43
- [13] Ellery A (2016) "Are self-replicating machines feasible?" *AIAA J Spacecraft & Rockets* 53 (2), 317-327
- [14] Bernold L (1994) "Cable-based lunar transportation system" *ASCE J Aerospace Engineering* 7 (1), 1-16
- [15] Dunbabin M, Corke P, Winstanley G, Roberts J (2006) "Off-world robotic excavation for large-scale habitat construction and resource extraction" *AAAI Spring Symp To Boldly Go Where No Human-Robot Team Has Gone Before*, Technical Report SS-07-6, Stanford, CA
- [16] Boles W, Ashley D, Tucker R (1993) "Lunar-base construction equipment and methods evaluation" *ASCE J Aerospace Engineering* 6, 217-235
- [17] Johnson L & King R (2010) "Measurement of force to excavate extraterrestrial regolith with a small bucket-wheel excavator" *J Terramechanics* 47, 87-95
- [18] Bland P, Artemieva N, Collins G, Bottke W, Bussey D, Joy K (2008) "Asteroids on the Moon: projectile survival during low velocity impacts" *39th Lunar & Planetary Science Conf*, abstract no 2045
- [19] Ellery A (2017) "Self-replicating machines: from theory to practice" *Proc Planetary & Terrestrial Mining Science Symp/Space Resources Roundtable*, paper no 1661
- [20] Bar-Cohen Y et al (2001) "Ultrasonic/sonic drilling/coring (USDC) for planetary application" *Proc SPIE 8th Annual Symposium on Smart Structures & Materials*, California, 4327-4355
- [21] Gao Y, Ellery A, Vincent J, Eckersley S, Jaddou M (2007) "Planetary micro-penetrator concept study with biomimetic drill and sampler design" *IEEE Trans Aerospace & Electronic Systems* 43 (3), 875-885
- [22] Satish H, Radziszewski P, Ouellet J (2005) "Design issues and challenges in lunar/Martian mining applications" *Mining Technology* 114 (2), 107-117
- [23] Nantel J (1996) "Improvements in mining technology" *Int Conf on Space Engineering, Construction & Operations in Space V*, Albuquerque, NM, 806-813
- [24] Costes N, Trautwein, W (1973) "Elastic loop mobility system - a new concept for planetary exploration" *J Terramechanics* 10(1), 89-104
- [25] A. Ellery (2005) "Robot-environment interaction - the basis for mobility in planetary micro-rovers" *Robotics & Autonomous Systems* 51, 29-39
- [26] A. Ellery & the Rover Team (2006) "ExoMars rover and Pasteur payload Phase A study: an approach to experimental astrobiology" *Int J Astrobiology* 5 (3), 221-241
- [27] D. Andrews, A. Colaprete, J. Quinn, D. Chavers, M. Picard, (2014) "Introducing the Resource Prospector Mission" *AIAA Space 2014 Conference & Exposition*, San Diego, California
- [28] Ellery A, Lowing P, Wanjara P, Kirby M, Mellor I, Doughty G (2017) "FFC Cambridge process with metal 3D printing as universal in-situ resource utilisation" *Proc Advanced Space Technology for Robotics & Automation (ASTRA)*, Leiden, Holland
- [29] Taylor L, Schmitt H, Carrier III D, Nakagawa M (2005) "Lunar dust problem: from liability to asset" *AIAA 1st Space Exploration Conf: Continuing the Voyage of Discovery*, Orlando FL, AIAA 2005-2510
- [30] Jones R, Haufe P, Sells E, Irvani P, Olliver V, Palmer C, Bowyer A (2011) "RepRap – the replicating rapid prototyper" *Robotica* 29 (Jan), 177-191
- [31] Taminger K & Hafley R (2006) "Electron beam freeform fabrication (EBF3) for cost-effective near-net shape manufacturing" NASA TM 2006-214284
- [32] Ciblak N & Lipkin H (1996) "Remote centre of compliance reconsidered" *Proc ASME Design Engineering Technical Conf & Computers in Engineering Conf*, Irvine, California, 1-20
- [33] Chen I-M (2001) "Rapid response manufacturing through a rapidly reconfigurable robotic workcell" *Robotics & Computer Integrated Manufacturing* 17, 199-213
- [34] Freitas R & Zachary W (1981) "Self-replicating growing lunar factory" *Proc 5th Princeton/AIAA Conf Space Manufacturing 4* (ed. Grey J & Hamdan L), AIAA Inc
- [35] Ellery A (2016) "John von Neumann's self-replicating machine – critical components required" *Proc IEEE Int Conf Systems Man & Cybernetics*, Budapest, Hungary, 314-319
- [36] Kunica Z, Vranjes B, Tomic I (2003) "Development of a design procedure for automatic assembly systems" *Proc IEEE Int Symp Assembly & Task Planning*, 295-300
- [37] Shukla C, Chen F (1996) "State of the art in intelligent real-time FMS control: a comprehensive survey" *J Intelligent Manufacturing* 7, 441-455
- [38] Lau H, Mak K (2001) "Extended unified framework for the rapid development of automated manufacturing systems" *Mechatronics* 11, 131-155
- [39] Zareba M, Morel G (2003) "Integration and control of

- intelligence in distributed manufacturing” *J Intelligent Manufacturing* **14**, 25-42
- [40] Huang S & Zhang H-C (1994) “Artificial neural networks in manufacturing: concepts, applications and perspectives” *IEEE Trans Components, Packaging & Manufacturing Technology – Part A* **17** (2), 212-228
- [41] Abdelhameed M & Tolbah F (2002) “Recurrent neural network-based sequential controller for manufacturing automated systems” *Mechatronics* **12**, 617-633
- [42] Monostori L (2003) “AI and machine learning techniques for managing complexity, changes and uncertainties in manufacturing” *Engineering Applications of Artificial Intelligence* **16**, 277-291
- [43] Mehrabi M, Ulsoy G, Koren Y (2000) “Reconfigurable manufacturing systems and their enabling technologies” *Int J Manufacturing Technology & Management* **1** (1), 114-131
- [44] Canny J, Goldberg K (1995) “RISC approach to sensing and manipulation” *J Robotic Systems* **12**, 351-363
- [45] Erdmann M, Mason M (1988) “Exploration of sensorless manipulation” *IEEE J Robotics & Automation* **4** (4), 369-379
- [46] Frosch R, Gallopoulos N (1989) “Strategies for manufacturing” *Scientific American* **261** (3), 144-152
- [47] Huang S, Liu P, Mokasadar A, Hou L (2013) “Additive manufacturing and its social impact: a literature review” *Int J Advanced Manufacturing Technology* **67**, 1191-1203
- [48] Huang R, Riddle M, Graziano D, Warren J, Das S, Nimbalkar S, Cresko J, Masanet E (2016) “Energy and emissions saving potential of additive manufacturing: the case of lightweight aircraft components” *J Cleaner Production* **135**, 1559-1570
- [49] Yang S, Zhao Y (2015) “Additive manufacturing-enabled design theory and methodology: a critical review” *Int J Advanced Manufacturing Technology* **80**, 327-342
- [50] Ford S, Despeisse M (2016) “Additive manufacturing and sustainability: an exploratory study of the advantages and challenges” *J Cleaner Production* **137**, 1573-1587
- [51] Campbell I, Bourell D, Gibson I (2012) “Additive manufacturing: rapid prototyping comes of age” *Rapid Prototyping J* **18** (4), 255-258
- [52] Ram J, Robinson C, Yang Y, Stucker B (2007) “Use of ultrasonic consolidation for fabrication of multi-material structures” *Rapid Prototyping J* **13** (4), 226-235
- [53] Obielodan J, Stucker B (2014) “Fabrication methodology for dual-material engineering structures using ultrasonic additive manufacturing” *Int J Advanced Manufacturing Technology* **70**, 277-284
- [54] Colombo P, Mera G, Riedel R, Soraru D (2010) “Polymer-derived ceramics: 40 years of research and innovation in advanced ceramics” *J American Ceramic Society* **93** (7), 1805-1837
- [55] Eckel Z, Zhou C, Martin J, Jacobsen A, Carter W, Schaedler T (2016) “Additive manufacturing of polymer-derived ceramics” *Science* **351** (Jan), 58-62
- [56] Ouyang M, Yuan C, Muisener R, Boulares A, Koberstein J (2000) “Conversion of some siloxane polymers to silicon oxide by UV/ozone photochemical processes” *Chemistry of Materials* **12**, 1591-1596
- [57] Greulich M, Greul M, Pintat T (1995) “Fast, functional prototypes via multiphase jet solidification” *Rapid Prototyping J* **1** (1), 20-25
- [58] Frazier W (2014) “Metal additive manufacturing: a review” *J Materials Engineering & Performance* **23**, 1917-1928
- [59] Bhavar V, Kattire P, Patil V, Khot S, Gujar K, Singh R (2016) “Review on powder bed fusion technology of metal additive manufacturing” in *Additive Manufacturing Handbook* (ed. Badiru A, Valencia V, Liu D), CRC Press, Boca Raton, FL, 251-262
- [60] Murr L (2015) “Metallurgy of additive manufacturing: examples from electron beam melting” *Additive Manufacturing* **5**, 40-53
- [61] Gu D, Meiners W, Wissenbach K, Poprawe R (2012) “Laser additive manufacturing of metallic components: materials, processes and mechanisms” *Int Materials Review* **57** (3), 133-164
- [62] Ding D, Pan Z, Cuiuri D, Li H (2015) “Wire feed additive manufacturing of metal components: technologies, developments and future interests” *Int J Advanced Manufacturing Technology* **81** (1), 465-481
- [63] Balla V, Roberson L, O’Connor G, Trigwell S, Bose S, Bandyopadhyay A (2011) “First demonstration on direct laser fabrication of lunar regolith parts” *Rapid Prototyping J* **18** (6), 451-457
- [64] Mueller R, Howe S, Kochmann D, Ali H, Anderson C, Burgoyne H, Chambers W, Clinton R, De Kestellier X, Ebelt K, Gerner S, Hofmann D, Hogstrom K, Ives E, Jerves A, Keeman R, Keravala J, Khoshnevis B, Lim S, Metzger P, Meza L, Nakaruma T, Nelson A, Partridge H, Pettit D, Pyle R, Reiners E, Shapiro A, Singer R, Tan W-L, Vasquez N, Wilcox B, Zelhofer A (2016) “Automated additive construction (AAC) for Earth and

- space using in-situ resources” *Proc 15th Biennial ASCE Int Conf Engineering Science Construction & Operations in Challenging Environments (Earth & Space 2016)*, Reston, VA
- [65] Eerton S, Hirsch M, Stravroulakis P, Leach R, Clare A (2016) “Review of in-situ process monitoring and in-situ metrology for metal additive manufacturing” *Materials & Design* **95**, 431-445
- [66] King W, Anderson A, Ferencz R, Hodge N, Kamath C, Khairallah S, Rubenchik A (2015) “Laser powder bed fusion additive manufacturing of metals: physics, computational and material challenges” *Applied Physics Review* **2**, 041304
- [67] Chirikjian G, Zhou Y, Suthakorn J (2002) “Self-replicating robots for lunar development” *IEEE/ASME Trans Mechatronics* **7** (4), 462-472
- [68] Moses M, Yamaguchi H, Chirikjian G (2009) “Towards cyclic fabrication systems for modular robotics and rapid manufacturing” *Robotics: Science & Systems V Conf*, University of Washington, Seattle
- [69] Ellery A (2016) “John von Neumann’s self-replicating machine – critical components required” *Proc IEEE Int Conf Systems Man & Cybernetics*, Budapest, Hungary, 314-319
- [70] Ellery A (2016) “Progress towards 3D printed mechatronic systems” *Proc IEEE Int Conf Industrial Technology with Symp on 3D Printing*, Tapei, Taiwan, pp. 1129-1133
- [71] Ellery A (2015) “Artificial intelligence through symbolic connectionism – a biomimetic rapprochement” in *Biomimetic Technologies: Principles & Applications* (ed. Ngo D), Elsevier Publishing
- [72] Schmidhuber J (2015) “Deep learning in neural networks: an overview” *Neural Networks* **61**, 85-117
- [73] Milford M & Wyeth G (2009) “Persistent navigation and mapping using a biologically inspired SLAM system” *Int J Robotics Research* **29** (9), 1131-1153
- [74] Rogers G, Bottaci L (1997) “Modular production systems: a new manufacturing paradigm” *J Intelligent Manufacturing* **8**, 147-156
- [75] Larson S & Ellery A (2015) “Trainable analogue neural network with application to lunar in-situ resource utilisation” *Proc Int Astronautics Federation Congress*, Jerusalem, IAC-15-D3.3.6
- [76] Lee K, Moses M, Chirikjian G (2008) “Robotic self-replication in structured environments: physical demonstrations and complexity measures” *Int J Robotics Research* **27** (3-4), 387-401
- [77] Cook S (1983) “Overview of computational complexity” *Communications ACM* **26** (6), 401-408
- [78] Woods D & Neary T (2009) “Complexity of small universal Turing machines: a survey” *Theoretical Computer Science* **410**, 443-450
- [79] Bennett C (1995) “Universal computation and physical dynamics” *Physica D* **86**, 268-273
- [80] Ben-Hur A, Siegelman H, Fishman S (2002) “Theory of complexity for continuous time systems” *J Complexity* **18**, 51-86

BIOGRAPHY



Alex Ellery received a BSc (Hons) Physics from the University of Ulster, UK (1988), MSc Astronomy from the University of Sussex, UK (1990) and PhD from Cranfield Institute of Technology, UK (1995). He is a graduate of the International Space University summer session (1993). He worked at Vickers Shipbuilding & Engineering Ltd UK as a systems design engineer, the Royal National Throat Nose & Ear Hospital London as a senior clinical scientist and Logica UK Ltd Space Division as a software engineer before embarking on an academic career at Queen Mary University of London UK as a programme manager on Herschel and Planck space telescopes, and Kingston University UK and then Surrey Space Centre UK as a senior lecturer specialized in space robotics. His current appointment is at Carleton University in Ottawa, Canada as a Canada Research Professor having spent a decade as a Canada Research Chair in Space Robotics & Space Technology. He is the author of two textbooks “An Introduction to Space Robotics” (2000) and “Planetary Rovers” (2016) both published by Praxis-Springer.